Machine Vision and Applications (2014) 25:185–197
DOI 10.1007/s00138-013-0511-3

ORIGINAL PAPER

Image-based magnification calibration for electron microscope

Koichi Ito · Ayako Suzuki · Takafumi Aoki · Ruriko Tsuneta

Received: 31 July 2012 / Revised: 7 February 2013 / Accepted: 2 April 2013 / Published online: 19 April 2013

Abstract Magnification calibration is a crucial task for the electron microscope to achieve accurate measurement of the target object. In general, magnification calibration is performed to obtain the correspondence between the scale of the electron microscope image and the actual size of the target object using the standard calibration samples. However, the current magnification calibration method mentioned above may include a maximum of 5 % scale error, since an alternative method has not yet been proposed. Addressing this problem, this paper proposes an image-based magnification calibration method for the electron microscope. The proposed method employs a multi-stage scale estimation approach using phase-based correspondence matching. Consider a sequence of microscope images of the same target object, where the image magnification is gradually increased so that the final image has a very large scale factor S (e.g., $S = 1{,}000$) with respect to the initial image. The problem considered in this paper is to estimate the overall scale factor S of the given image sequence. The proposed scale estimation method provides a new methodology for high-accuracy magnification calibration of the electron microscope. This paper also proposes a quantitative performance evaluation method of scale estimation algorithms using Mandelbrot images which are precisely scale-controlled images. Experimental evaluation using Mandelbrot images shows that the proposed scale estimation algorithm can estimate the overall scale factor $S = 1{,}000$ with approximately 0.1 % scale error. Also, a set of experiments using image sequences taken by an actual scanning transmission electron microscope (STEM) demonstrates that the proposed method is more effective for magnification calibration of a STEM compared with a conventional method.

Keywords Scale estimation · Image matching · Correspondence matching · Electron microscope · Phase-only correlation

K. Ito (✉) · A. Suzuki · T. Aoki
Graduate School of Information Sciences, Tohoku University, 6-6-05, Aramaki Aza Aoba, Sendai 980-8579, Japan
e-mail: ito@aoki.ecei.tohoku.ac.jp

R. Tsuneta
Hitachi, Ltd., Central Research Laboratory, 1-280, Higashi-Koigakubo, Kokubunji 185-8601, Japan

1 Introduction

Electron microscopes can be used to measure and observe cells, cell organelle, the fine structure of biological membranes, atoms, etc., and have a 1,000 times greater resolution than light microscopes. To achieve accurate measurement and observation of the object using electron microscope images, the correspondence between the scale of the electron microscope image and the actual size of the object must be obtained. This task is known as magnification calibration of the electron microscope. The high-accuracy magnification calibration method is required for accurate measurement and observation of the object.

In general, magnification calibration is performed using standard calibration samples containing line, grating or spherical patterns with known spacing [1,4,7,12,13]. For example, microscopic glass spheres [4], polystyrene latex spheres [1], polyoma and a spherical animal virus [12], crystals of bovine liver catalase [7], monodisperse gold nanoparticles [13], carbon gratings and carbon graphites are used as the internal or external standard calibration samples. The internal standard calibration sample such as an atomic pattern of the target object is included in the target object and is used to simultaneously calibrate the magnification and measure the

target object, while the external one such as a grating pattern is not included in the target object and is used to calibrate the magnification in advance. In the basic calibration method, a carbon grating is used in the low magnification setting (i.e., μm order), and an atomic lattice of the target object is used in the high magnification setting (i.e., nm order). When we focus on the magnification range between these two magnification settings, there are no applicable standard materials. Hence, it is difficult to perform reliable magnification calibration of the electron microscope over this range, and the current magnification calibration method using the standard calibration samples may include a maximum of 5 % scale error [11]. In addition, an alternative method has not yet been proposed.

Addressing this problem, we propose a novel framework of magnification calibration using a multi-stage scale estimation approach. We consider a sequence of microscope images of the same target object, where the image magnification is gradually increased so that the final image has a very large scale factor S (e.g., $S = 1{,}000$) with respect to the initial image. The goal of this framework is to estimate the overall scale factor S between the image captured with the correct magnification setting and the image captured with the uncalibrated magnification setting. Since the overall scale factor S is obtained by the product of a sequence of estimated relative scale factors, a high-accuracy scale estimation algorithm for estimating the relative scale factors between adjacent images is indispensable. Moreover, in high-magnification range over $\times$ 100,000, the geometric transformation between sequential images is represented by not only scaling but also translation, rotation and sometimes perspective distortion due to slight movement of the object during image acquisition, which is known as drift distortion. Hence, a scale estimation algorithm has to be robust against geometric transformation. To achieve high-accuracy magnification calibration of the electron microscope, we propose a high-accuracy scale estimation algorithm using correspondence matching based on phase-only correlation (POC). Phase-based correspondence matching [10] is an efficient method of sub-pixel correspondence matching, which employs (1) a coarse-to-fine strategy using image pyramids for robust correspondence search and (2) a POC-based sub-pixel image matching technique for finding a pair of corresponding points with sub-pixel displacement accuracy.

In addition, to evaluate the accuracy of scale estimation algorithms, we propose a quantitative performance evaluation method of scale estimation algorithms using Mandelbrot images. The Mandelbrot set [3] is a mathematical set of points having distinctive boundaries and two-dimensional (2D) fractal-like shape. Considering the Mandelbrot set as 2D signals defined in the continuous space, we can generate images transformed with arbitrary parameters without interpolating pixels, since the Mandelbrot set has infinite resolution. The use of Mandelbrot images makes it possible to generate the image sequence with a very large scale factor S (e.g., $S = 1{,}000$).

Experimental evaluation using Mandelbrot images as precisely scale-controlled images shows that the proposed scale estimation algorithm can estimate the scale factor with approximately 0.1 % scale accuracy from the image sequences with the overall scale factor $S = 1{,}000$ and ± 10 % of the initial scale errors. This paper also describes an application of the proposed algorithm to the magnification calibration of an actual scanning transmission electron microscope (STEM).

The main contributions of this work are summarized as follows:

1. A novel framework of magnification calibration using a multi-stage scale estimation approach for electron microscopes is proposed. The proposed framework allows us to perform magnification calibration of electron microscopes within the magnification range for which no applicable standard materials exist.
2. A scale estimation algorithm using the phase-based correspondence matching technique is proposed. The proposed algorithm can estimate the overall scale factor $S = 1{,}000$ with approximately 0.1 % scale error.
3. A quantitative performance evaluation method using Mandelbrot images for scale estimation algorithms is proposed. Since the proposed method generates the image sequences whose scale factors are precisely controlled, we can correctly evaluate the accuracy of scale estimation algorithms even for the overall scale factor $S = 1{,}000$.

The rest of the paper is organized as follows: Section 2 describes the proposed image-based magnification calibration framework for electron microscopes. Section 3 describes the fundamentals of POC, the phase-based correspondence matching technique and the proposed scale estimation algorithm. Section 4 describes the use of Mandelbrot image for quantitative evaluation of scale estimation algorithms. Section 5 demonstrates a set of experiments for evaluating estimation accuracy of the proposed algorithm using Mandelbrot images and the images taken by an actual STEM. Section 6 ends with some concluding remarks.

2 Image-based magnification calibration

In this section, we describe a novel framework of magnification calibration using a multi-stage scale estimation approach for electron microscopes. Figure 1 shows the flow of our proposed framework.

We assume that the electron microscope has already been calibrated for a certain magnification setting m_0^{true} (>1)

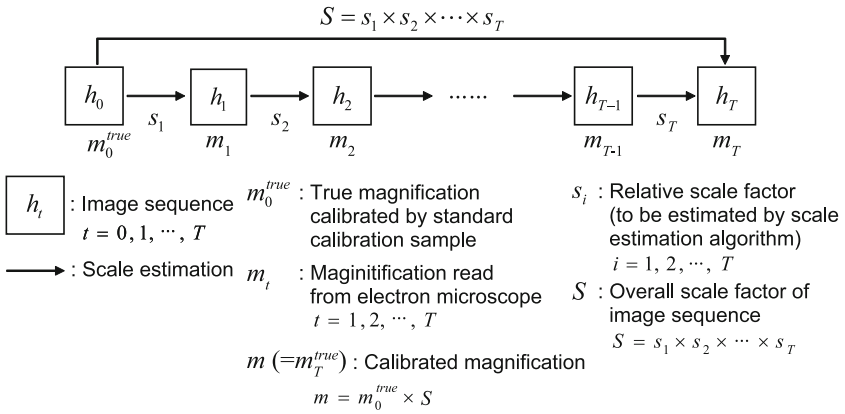

Fig. 1 Scheme of the proposed image-based magnification calibration: It is hard to estimate a very large overall scale factor S between the initial image h_0 and target image h_T directly. The proposed framework estimates the overall scale factor S through a multi-step approach as $S = s_1 \times s_2 \times s_3 \times \cdots \times s_T$, where we employ a set of multiple images between h_0 and h_T with reasonably smaller relative scale factors s_i $(i = 1, 2, 3, \ldots, T)$. We can calibrate the magnification of the target image h_t as $m = m_0^{\text{true}} \times S$ by estimating the accurate relative scale factors s_i

using standard calibration samples, and hence the magnification parameter m_0^{true} has been adjusted correctly. The problem considered here is to calibrate the microscope for a higher magnification setting, say m $(>m_0^{\text{true}})$, for which no standard calibration materials exist. Our framework is to estimate the scale change S between the microscope image h_0 captured with the correct magnification setting m_0^{true} and the target image h_T captured with the uncalibrated magnification setting m_T. Let S (>1) be the scale factor of the microscope image h_T with respect to the image h_0. We can estimate the true magnification for the setting m $(=m_T^{\text{true}})$ as $S \times m_0^{\text{true}}$. Thus, the goal of our framework is to perform calibration for magnification m on the basis of image analysis without using standard calibration materials.

A major problem of this framework is the difficulty of calibration for higher magnification setting m $(>> m_0^{\text{true}})$. For example, when $S = m/m_0^{\text{true}} = 1{,}000$, we cannot estimate the image scale factor S directly in practice. Addressing this problem, we estimate the overall scale factor S through a multi-step approach as $S = s_1 \times s_2 \times s_3 \times \cdots \times s_T$, where we employ a set of multiple images between h_0 and h_T with reasonably smaller relative scale factors s_i $(i = 1, 2, 3, \ldots, T)$. Hence, high-accuracy scale estimation for the relative scale factor s_i between h_{t-1} and h_t is indispensable to reduce the multiplicative error accumulation including in the overall scale factor S. In the following section, we describe a high-accuracy scale estimation algorithm using phase-based correspondence matching.

3 Scale estimation algorithm

A number of image matching algorithms to estimate transformation parameters have been proposed. One of the famous image matching algorithms is to use scale invariant feature transform (SIFT)-based matching [6]. In the case of computer vision applications, SIFT-like feature-based matching algorithms exhibit sufficient accuracy to estimate transformation parameters [8]. However, for the purpose of scale estimation in microscope images, SIFT-like feature-based matching algorithms are not always suitable, since only one-pixel error of keypoint localization may lead to a significant error in scale estimation. Hence, for the cases considered in this paper, area-based image matching algorithms are more suitable than the feature-based image matching algorithms. The area-based image matching algorithm using POC is one of the most accurate algorithms to estimate transformation parameters such as translational displacement, rotation angle and scale factor [5,9]. POC is an image matching technique using the phase components of 2D Discrete Fourier Transforms (DFTs) of given images. To combine the POC technique and the Fourier–Mellin transform, we can estimate a scale factor between images [2,9]. Since this approach estimates a scale factor from the amplitude components of 2D DFTs of images, the low-quality images due to blur or noise, e.g., microscope images in high-magnification settings, result in a reduction of the accuracy of scale estimation.

To achieve accurate scale estimation of electron microscope images, the proposed scale estimation algorithm obtains dense correspondence between images using a correspondence matching technique, and then estimates the scale factor from the correspondence. The key idea of the proposed algorithm is to use phase-based correspondence matching [10], which employs (1) a coarse-to-fine strategy using image pyramids for robust correspondence search and (2) a POC-based sub-pixel image matching technique for finding a pair of corresponding points with sub-pixel displacement accuracy. In the following, we describe the details of the pro-

posed scale estimation algorithm. First, we briefly introduce fundamentals of POC, which allows us to estimate a sub-pixel displacement and evaluate a similarity between two images. Next, we describe the correspondence matching technique using POC. Then, we describe the proposed scale estimation algorithm using phase-based correspondence matching.

3.1 Fundamentals of phase-only correlation

POC-based image matching employs a POC function between two images which is defined by a correlation function calculated only from phase components in 2D DFTs of the given images. Consider two $N_1 \times N_2$ images, $f(n_1, n_2)$ and $g(n_1, n_2)$, where we assume that the index ranges are $n_1 = -M_1, \ldots, M_1\,(M_1 > 0)$ and $n_2 = -M_2, \ldots, M_2\,(M_2 > 0)$, and hence $N_1 = 2M_1 + 1$ and $N_2 = 2M_2 + 1$. Note that we assume here the sign symmetric index ranges $\{-M_1, \ldots, M_1\}$ and $\{-M_2, \ldots, M_2\}$ for mathematical simplicity. The discussion could be easily generalized to non-negative index ranges with power-of-two image size. Let $F(k_1, k_2)$ and $G(k_1, k_2)$ denote the 2D DFTs of the two images. $F(k_1, k_2)$ and $G(k_1, k_2)$ are given by

$$\begin{aligned} F(k_1, k_2) &= \sum_{n_1=-M_1}^{M_1} \sum_{n_2=-M_2}^{M_2} f(n_1, n_2) W_{N_1}^{k_1 n_1} W_{N_2}^{k_2 n_2} \\ &= A_F(k_1, k_2) e^{j\theta_F(k_1,k_2)}, \end{aligned} \tag{1}$$

$$\begin{aligned} G(k_1, k_2) &= \sum_{n_1=-M_1}^{M_1} \sum_{n_2=-M_2}^{M_2} g(n_1, n_2) W_{N_1}^{k_1 n_1} W_{N_2}^{k_2 n_2} \\ &= A_G(k_1, k_2) e^{j\theta_G(k_1,k_2)}, \end{aligned} \tag{2}$$

where $k_1 = -M_1, \ldots, M_1$, $k_2 = -M_2, \ldots, M_2$, $W_{N_1} = e^{-j\frac{2\pi}{N_1}}$, and $W_{N_2} = e^{-j\frac{2\pi}{N_2}}$. $A_F(k_1, k_2)$ and $A_G(k_1, k_2)$ are amplitude components, and $\theta_F(k_1, k_2)$ and $\theta_G(k_1, k_2)$ are phase components. The normalized cross-power spectrum $R_{FG}(k_1, k_2)$ between $F(k_1, k_2)$ and $G(k_1, k_2)$ is given by

$$\begin{aligned} R_{FG}(k_1, k_2) &= \frac{F(k_1, k_2)\overline{G(k_1, k_2)}}{|F(k_1, k_2)\overline{G(k_1, k_2)}|} \\ &= e^{j\theta(k_1,k_2)}, \end{aligned} \tag{3}$$

where $\overline{G(k_1, k_2)}$ denotes the complex conjugate of $G(k_1, k_2)$ and $\theta(k_1, k_2)$ denotes the phase difference $\theta_F(k_1, k_2) - \theta_G(k_1, k_2)$. The POC function $r_{fg}(n_1, n_2)$ is the 2D Inverse DFT of $R_{FG}(k_1, k_2)$ and is given by

$$\begin{aligned} r_{fg}(n_1, n_2) = \frac{1}{N_1 N_2} \sum_{k_1=-M_1}^{M_1} \sum_{k_2=-M_2}^{M_2} & R_{FG}(k_1, k_2) \\ & \times W_{N_1}^{-k_1 n_1} W_{N_2}^{-k_2 n_2}. \end{aligned} \tag{4}$$

When the two images are similar, their POC function gives a distinct sharp peak. When $f(n_1, n_2) = g(n_1, n_2)$, the POC function r_{fg} becomes the Kronecker delta function. When the two images are not similar, the peak drops significantly. The height of the peak can be used as a good similarity measure for image matching, and the location of the peak shows the translational displacement between the two images. Other important properties of POC are that the POC-based image matching is not influenced by image shift or brightness change, and it is highly robust against noise.

In our previous work [9], we have proposed techniques to improve the accuracy of POC-based image matching: (1) the function fitting technique for high-accuracy estimation of peak position, (2) the windowing technique to reduce boundary effects and (3) the spectral weighting technique to reduce aliasing and noise effects. Technique (1) is to find the location of the peak that may exist between pixels by fitting the closed-form peak model of the POC function. Technique (2) is to reduce the effects of discontinuity at the image border in the 2D DFT computation by applying a 2D window function to the image. Technique (3) is to eliminate the high frequency components having low reliability by applying a low-pass-type weighting function to $R_{FG}(k_1, k_2)$ in the frequency domain. The use of POC-based image matching with the above three techniques makes it possible to achieve accurate and robust estimation of translational displacement between images.

3.2 Phase-based correspondence matching

To perform accurate scale estimation, we employ the sub-pixel correspondence matching technique using POC, which employs (1) a coarse-to-fine strategy using image pyramids for robust correspondence search and (2) a sub-pixel translational displacement estimation method using POC for finding a pair of corresponding points with sub-pixel displacement accuracy. The flow of the phase-based correspondence matching technique is illustrated in Fig. 2. Consider two images: the reference image $I(n_1, n_2)$ and the input image $J(n_1, n_2)$. Let $\boldsymbol{p}$ be a coordinate vector of a reference pixel in $I(n_1, n_2)$. The problem of sub-pixel correspondence search is to find a real-number coordinate vector $\boldsymbol{q}$ in $J(n_1, n_2)$ that corresponds to the reference pixel $\boldsymbol{p}$ in $I(n_1, n_2)$. We briefly explain the procedure as follows.

Step 1 For $l = 1, 2, \ldots, l_{\max} - 1$, create the lth layer images $I^l(n_1, n_2)$ and $J^l(n_1, n_2)$, i.e., coarser versions of $I^0(n_1, n_2)$ and $J^0(n_1, n_2)$, recursively as follows:

$$I^l(n_1, n_2) = \frac{1}{4} \sum_{i_1=0}^{1} \sum_{i_2=0}^{1} I^{l-1}(2n_1 + i_1, 2n_2 + i_2),$$

$$J^l(n_1, n_2) = \frac{1}{4} \sum_{i_1=0}^{1} \sum_{i_2=0}^{1} J^{l-1}(2n_1 + i_1, 2n_2 + i_2).$$

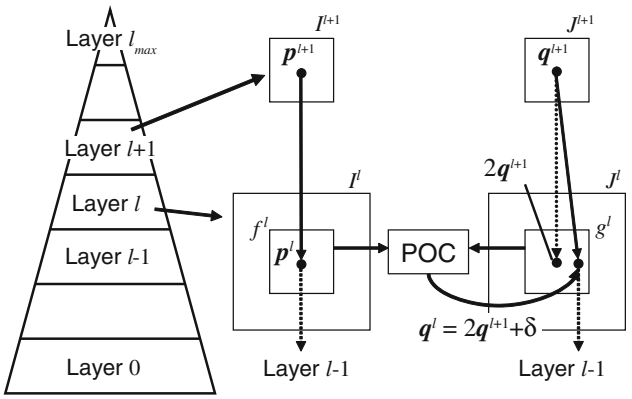

Fig. 2 Flow of the phase-based correspondence matching technique: We put the reference point $\boldsymbol{p}$ on the reference image $I(n_1, n_2)$ and find its corresponding point $\boldsymbol{q}$ on the input image $J(n_1, n_2)$ as follows. Create lth layer images $I^l(n_1, n_2)$ and $J^l(n_1, n_2)$ recursively. Calculate $\boldsymbol{p}^l$ corresponding to $\boldsymbol{p}^0$. Assume $\boldsymbol{p}^{l_{\max}} = \boldsymbol{q}^{l_{\max}}$ in the coarsest layer. For the lth layer images, extract sub-images $f^l(n_1, n_2)$ and $g^l(n_1, n_2)$ with their centers on $\boldsymbol{p}^l$ and $2\boldsymbol{q}^{l+1}$, respectively. Estimate the displacement $\boldsymbol{\delta}^l$ between $f^l(n_1, n_2)$ and $g^l(n_1, n_2)$ with pixel accuracy using POC-based image matching and obtain the lth layer corresponding point as $\boldsymbol{q}^l = 2\boldsymbol{q}^{l+1} + \boldsymbol{\delta}^l$. Repeat the above procedure while $l \geq 0$. In the original images $I^0(n_1, n_2)$ and $J^0(n_1, n_2)$, estimate the displacement $\boldsymbol{\delta}$ between two sub-images with their centers on $\boldsymbol{p}^l$ and $2\boldsymbol{q}^{l+1}$. Finally, obtain the corresponding point as $\boldsymbol{q} = \boldsymbol{q}^0 + \boldsymbol{\delta}$

In this paper, we employ $l_{\max} = 3$.

Step 2 For every layer $l = 1, 2, \ldots, l_{\max}$, calculate the coordinate $\boldsymbol{p}^l = (p_1^l, p_2^l)$ corresponding to the original reference point $\boldsymbol{p}^0$ recursively as follows:

$$\boldsymbol{p}^l = \left\lfloor \tfrac{1}{2}\boldsymbol{p}^{l-1} \right\rfloor = \left(\left\lfloor \tfrac{1}{2}p_1^{l-1} \right\rfloor, \left\lfloor \tfrac{1}{2}p_2^{l-1} \right\rfloor \right), \tag{5}$$

where $\lfloor z \rfloor$ denotes the operation to round the element of z to the nearest integer towards minus infinity.

Step 3 We assume that $\boldsymbol{q}^{l_{\max}} = \boldsymbol{p}^{l_{\max}}$ in the coarsest layer. Let $l = l_{\max} - 1$.

Step 4 From the lth layer images $I^l(n_1, n_2)$ and $J^l(n_1, n_2)$, extract two sub-images (or local image blocks) $f^l(n_1, n_2)$ and $g^l(n_1, n_2)$ with their centers on $\boldsymbol{p}^l$ and $2\boldsymbol{q}^{l+1}$, respectively. The size of image blocks is $W \times W$ pixels. Note that W is determined depending on the image size. Consider the images with 640×480 pixels and $l_{\max} = 3$. The image size in the $(l_{\max} - 1)$th layer is 160×120 pixels. W should be smaller than 120 pixels so as not to extract the sub-images from outside of the image, and also be power of two for fast DFT computation. The candidates for W are 32 and 64 pixels to estimate accurate displacement between the two sub-images using POC-based image matching. From the viewpoint of computation time, we employ $W = 32$ in this paper. If the image size is over $1{,}000 \times 1{,}000$ pixels, it is better to select $W = 64$.

Step 5 Estimate the displacement between $f^l(n_1, n_2)$ and $g^l(n_1, n_2)$ with pixel accuracy using POC-based image matching. Note that, to reduce the computational cost, POC-based image matching with pixel-accuracy is used to estimate the displacement in this step, since $f^l(n_1, n_2)$ and $g^l(n_1, n_2)$ are the coarser versions of the original images $f^0(n_1, n_2)$ and $g^0(n_1, n_2)$. Let the estimated displacement vector be $\boldsymbol{\delta}^l$. The lth layer correspondence $\boldsymbol{q}^l$ is determined by

$$\boldsymbol{q}^l = 2\boldsymbol{q}^{l+1} + \boldsymbol{\delta}^l. \tag{6}$$

Step 6 Decrement the counter by 1 as $l = l - 1$ and repeat the procedure from Step 4 to Step 6 while $l \geq 0$.

Step 7 From the original images $I^0(n_1, n_2)$ and $J^0(n_1, n_2)$, extract two image blocks with their centers on $\boldsymbol{p}^0$ and $\boldsymbol{q}^0$, respectively. Estimate the displacement between the two blocks with sub-pixel accuracy using POC-based image matching. Let the estimated displacement vector with sub-pixel accuracy be denoted by $\boldsymbol{\delta} = (\delta_1, \delta_2)$. Update the corresponding point as

$$\boldsymbol{q} = \boldsymbol{q}^0 + \boldsymbol{\delta}. \tag{7}$$

In general, it is important to set the reference point $\boldsymbol{p}$ on the area having rich texture to obtain its accurate corresponding point $\boldsymbol{q}$ from the input image $J(n_1, n_2)$. Since the peak value of the POC function between the local block images is used as a measure of correspondence reliability [9], a lot of reference points $\boldsymbol{p}$ are placed on the reference image $I(n_1, n_2)$ and their corresponding points $\boldsymbol{q}$ on the input image $J(n_1, n_2)$ are found using the phase-based correspondence matching technique described in the above. When the peak value of the POC function between the local image blocks is below a threshold, the corresponding point pair is regarded as an outlier. From our preliminary investigation, the threshold is selected within 0.3–0.5 to obtain accurate corresponding point pairs. Hence, we employ the threshold as 0.4 in this paper. Also, we empirically determine that the reference points are set on the reference image with a spacing of 10 pixels.

3.3 Scale estimation algorithm using phase-based correspondence matching

We present a scale estimation algorithm using phase-based correspondence matching for electron microscope images. As mentioned in Sect. 2, the problem considered here is to estimate the precise relative scale factor s_t $(t = i)$ between the two neighboring images $h_t(n_1, n_2)$ and $h_{t-1}(n_1, n_2)$ of the image sequence as shown in Fig. 3. Let $h_t(n_1, n_2)$ and $h_{t-1}(n_1, n_2)$ be the high-magnification image with the magnification m_t and the low-magnification image with the magnification m_{t-1}, respectively. Note that the magnification m_t and m_{t-1} are read from the electron microscope. The relative scale factor s_t can be written as

$$s_t = \tilde{s}_t + \Delta s_t, \tag{8}$$

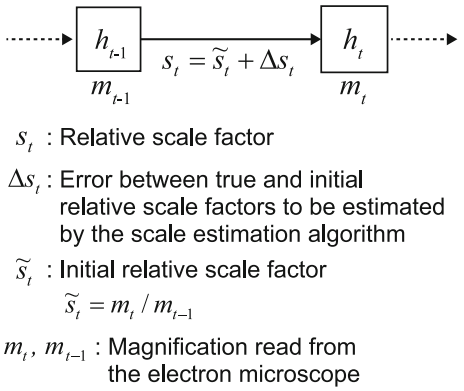

Fig. 3 Flow diagram of estimating the relative scale factor s_t between the two neighboring images h_t and h_{t-1}: From the magnification m_t of the high-magnification image $h_t(n_1, n_2)$ and m_{t-1} of the low-magnification image $h_{t-1}(n_1, n_2)$, the initial scale factor $\tilde{s}_t$ is defined by $\tilde{s}_t = m_t/m_{t-1}$. The initial scale factor $\tilde{s}_t$ includes the error between the true and initial relative scale factors denoted by Δs_t, i.e., the error including in the magnification read from the electron microscope. We need to estimate Δs_t with high accuracy using a scale estimation algorithm to obtain the precise relative scale factor s_t defined by $s_t = \tilde{s}_t + \Delta s_t$

where $\tilde{s}_t$ indicates the initial scale factor $\tilde{s}_t$ defined by $\tilde{s}_t = m_t/m_{t-1}$ and Δs_t indicates the error between the true and initial relative scale factors, i.e., the error included in the magnification read from the electron microscope which may be a maximum of 5 % [11]. Hence, we need to estimate Δs_t with high accuracy to obtain the precise relative scale factor s_t. In the proposed algorithm, we consider that $h_{t-1}(n_1, n_2)$ is a displaced, rotated and scaled version of the image $h_t(n_1, n_2)$, since the electron microscope image may be deformed in the image acquisition process. In high-magnification range over $\times 100{,}000$, the geometric transformation between the images is represented by not only scaling but also translation, rotation and sometimes perspective distortion due to slight movement of the object during image acquisition, which is known as drift distortion. Hence, the proposed algorithm estimates the relative scale factor s_t in the light of the translational displacement $(\delta_{t1}, \delta_{t2})$ and rotation angle θ_t between images. Also, we employ the iterative procedure to estimate the relative scale factor s_t between $h_t(n_1, n_2)$ and $h_{t-1}(n_1, n_2)$. If the initial relative scale factor $\tilde{s}_t$ includes a large error, one-time correspondence matching may not be enough to obtain the accurate relative scale factor s_t. In the proposed algorithm, the parameters s_t, θ_t and $(\delta_{t1}, \delta_{t2})$ are iteratively estimated. The following is the detailed procedure of the proposed algorithm (Fig. 4).

Input:

- High-magnification image $h_t(n_1, n_2)$ with the magnification m_t read from the electron microscope
- Low-magnification image $h_{t-1}(n_1, n_2)$ with the magnification m_{t-1} read from the electron microscope

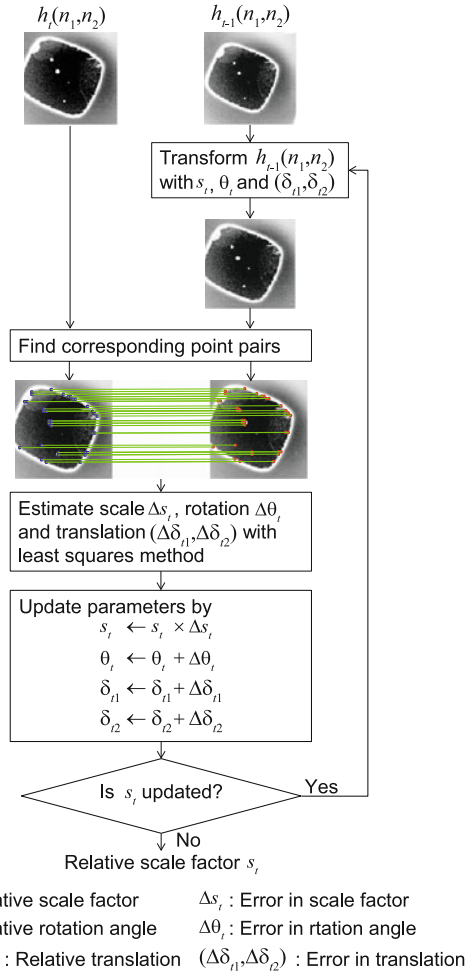

Fig. 4 Flow diagram of the proposed scale estimation algorithm: If the initial relative scale factor $\tilde{s}_t$ includes a large error, one-time correspondence matching may not be enough to obtain the accurate relative scale factor s_t. In the proposed algorithm, the parameters such as the relative scale factor s_t, the relative rotation angle θ_t and the relative translation $(\delta_{t1}, \delta_{t2})$ between $h_t(n_1, n_2)$ and $h_{t-1}(n_1, n_2)$ are iteratively estimated so as to minimize errors in scale factor Δs_t, rotation angle $\Delta\theta_t$ and translation $(\Delta\delta_{t1}, \Delta\delta_{t2})$

- Initial value $\tilde{s}_t = m_t/m_{t-1}$ of the relative scale factor s_t between $h_t(n_1, n_2)$ and $h_{t-1}(n_1, n_2)$

Output:

- Relative scale factor s_t between $h_t(n_1, n_2)$ and $h_{t-1}(n_1, n_2)$.

Step 1 Set the initial transformation parameters, i.e., the translational displacement $(\delta_{t1}, \delta_{t2})$, the rotation angle θ_t and the scale factor s_t, as follows:

$$(\delta_{t1}, \delta_{t2}) \leftarrow (0, 0),$$
$$\theta_t \leftarrow 0,$$
$$s_t \leftarrow \tilde{s}_t.$$

Step 2 Transform $h_{t-1}(n_1, n_2)$ by $(\delta_{t1}, \delta_{t2})$, θ_t and s_t, and extract the common region $h'_{t-1}(n_1, n_2)$ associated with $h_t(n_1, n_2)$.

Step 3 Obtain the correspondence between $h_t(n_1, n_2)$ and $h'_{t-1}(n_1, n_2)$ using the phase-based correspondence matching technique described in Sect. 3.2. In this paper, we set the reference points on $h_t(n_1, n_2)$ with a spacing of 10 pixels. When the peak value of POC function between local block images is below a certain threshold, the point pair is regarded as an outlier, and is removed. In this paper, the threshold value is 0.4. Let the reference points be $\boldsymbol{U} = (\boldsymbol{u}_1, \boldsymbol{u}_2, \ldots, \boldsymbol{u}_K)$ for $h_t(n_1, n_2)$ and the corresponding points be $\boldsymbol{V} = (\boldsymbol{v}_1, \boldsymbol{v}_2, \ldots, \boldsymbol{v}_K)$ for $h'_{t-1}(n_1, n_2)$, where K is the number of corresponding point pairs.

Step 4 Estimate the scale error Δs_t using the correspondence between $h_t(n_1, n_2)$ and $h'_{t-1}(n_1, n_2)$. In this paper, we employ the similarity transformation model to estimate Δs_t. The model is defined as follows:

$$\boldsymbol{v} = \Delta s_t \begin{bmatrix} \cos \Delta\theta_t & -\sin \Delta\theta_t \\ \sin \Delta\theta_t & \cos \Delta\theta_t \end{bmatrix} \boldsymbol{u} + \begin{bmatrix} \Delta\delta_{t1} \\ \Delta\delta_{t2} \end{bmatrix}, \tag{9}$$

where $\Delta\theta_t$ is a rotation angle and $(\Delta\delta_{t1}, \Delta\delta_{t2})$ is a translational displacement. Substituting $\boldsymbol{U}$ and $\boldsymbol{V}$ into Eq. (9), we can estimate the transformation parameters by solving a set of linear simultaneous equations as the linear least-squares problem (For more details, refer to Appendix A in Ref. [8]).

Step 5 Update the transformation parameters as follows:

$$\begin{aligned} (\delta_{t1}, \delta_{t2}) &\leftarrow (\delta_{t1} + \Delta\delta_{t1}, \delta_{t2} + \Delta\delta_{t2}), \\ \theta_t &\leftarrow \theta_t + \Delta\theta_t, \\ s_t &\leftarrow s_t \times \Delta s_t, \end{aligned}$$

where "$\times$" indicates regular multiplication.

Step 6 Repeat the procedure from Step 2 to Step 5 until s_t is not updated. In this paper, we repeat the procedure 3 times.

Step 7 Obtain the relative scale factor s_t.

For every neighboring image pair, the precise relative scale factor s_i $(i = 1, \ldots, T)$ is estimated using the above scale estimation algorithm, and then the overall scale factor of the image sequence is obtained by $S = s_1 \times s_2 \times \cdots s_T$. Finally, we can calibrate the magnification of the image $h_T(n_1, n_2)$ by $m = m_0^{\text{true}} \times S$.

4 Mandelbrot image for quantitative performance evaluation of scale estimation

This section describes the proposed performance evaluation method for scale estimation. The reference images transformed with known parameters have to be used to evaluate the accuracy of image registration algorithms. For example, to obtain reference images with sub-pixel translation, we apply a lowpass filter to a high-resolution image and downsample shifted versions of the image. Using appropriate downsampling rates, we can generate the images having sub-pixel translation. On the other hand, pixel interpolation is required to generate the images with rotation and scaling. We can also obtain translated, rotated and scaled images, where an object is mounted on a micro stage which allows precise alignment of the object position and is taken by a camera. In this case, we need a precise micro stage and to carefully operate the camera and stage to reduce the error associated with human and device. Particularly, it is difficult to generate the image having a very large scale factor S, e.g., $S > 1{,}000$.

In this paper, we propose a performance evaluation method using the Mandelbrot set [3] for scale estimation algorithms. Figure 5 shows an example of the Mandelbrot set. The Mandelbrot set is a set of points in the complex plane having elaborate boundaries, where the little copies of the Mandelbrot set are connected to the main body of the set and are all slightly different. Considering the Mandelbrot set as 2D signals defined in the continuous space, we can generate the images transformed with arbitrary parameters

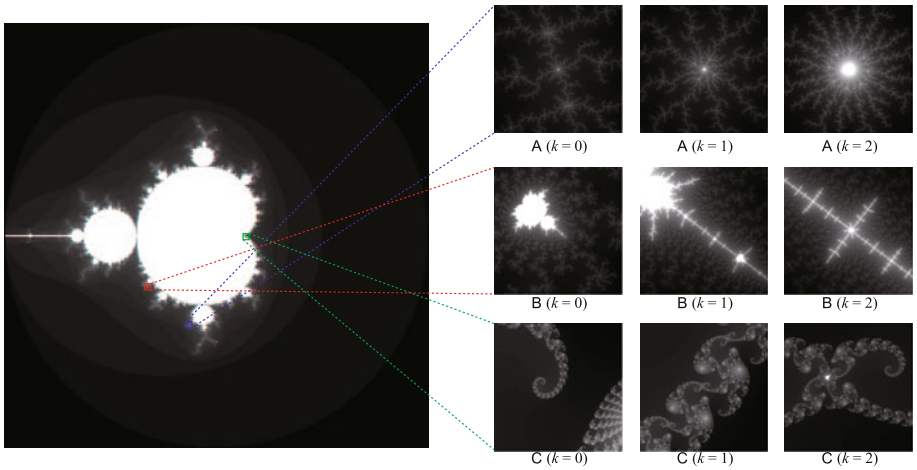

Fig. 5 The whole structure of the Mandelbrot set (*left*) and examples of Mandelbrot images (*right*) generated by changing the image centers (c_1, c_2) and the scale parameter k, where A, B and C indicate the parameter set used to generate each Mandelbrot image

without interpolating pixels, since the Mandelbrot set has infinite resolution.

We describe a Mandelbrot image generation procedure in the following. The Mandelbrot set defined as the set of complex values of $x_1 + jx_2$ is obtained from the following quadratic recurrence equation as follows:

$$z_{n+1} = z_n^2 + x_1 + jx_2, \tag{10}$$

where x_1 and x_2 are real-number coordinates, and the initial condition is $z_0 = 0$. In nature, the Mandelbrot set is the set of all points in the complex plain $x_1 + jx_2$ which do not diverge under $n \to \infty$. To reduce the computational cost, we calculate Eq. (10) up to $n = U$, where $U = 1{,}000$ in this paper. If $|z_n| \geq 2\,(n \leq U)$, the intensity value $h_c(x_1, x_2)$ for (x_1, x_2) in the complex plain is n. If $|z_n| \leq 2$ until $n = U$, the intensity value $h_c(x_1, x_2)$ is U. Thus, we can obtain the Mandelbrot set as $h_c(x_1, x_2)$. Note that we employ $h'_c(x_1, x_2) = \log\{h_c(x_1, x_2) + 1\}$ instead of $h_c(x_1, x_2)$ for intensity compression.

The Mandelbrot set $h'_c(x_1, x_2)$ can be considered as a 2D image defined in the continuous space. We now sample the continuous Mandelbrot set $h'_c(x_1, x_2)$ at the sampling intervals T_1 and T_2 to have a Mandelbrot image $h(n_1, n_2)$. Let (c_1, c_2) be image centers and (n_1, n_2) be discrete space indices, we have

$$h(n_1, n_2) = h'_c(x_1 - c_1, x_2 - c_2)|_{x_1 = n_1 T_1, x_2 = n_2 T_2}, \tag{11}$$

where $n_1 = -M_1, \ldots, M_1$ and $n_2 = -M_2, \ldots, M_2$. Figure 5 shows examples of Mandelbrot images generated by changing image centers (c_1, c_2) and the scale parameter k. In these figures, we employ the three patterns as follows:

$$\begin{aligned}
\text{A}: \ & D = 1.0 \times 10^{-11}, \\
& c_1 = -0.25272149866535, \\
& c_2 = 0.84996890117939, \\
\text{B}: \ & D = 1.0 \times 10^{-7}, \\
& c_1 = -0.64868627955000, \\
& c_2 = 0.48617790435000, \\
\text{C}: \ & D = 5.0 \times 10^{-6}, \\
& c_1 = 0.28950114650000, \\
& c_2 = 0.01346307350000,
\end{aligned}$$

where $T_1 = T_2 = D \times 10^k$ $(k = 0, 1, 2)$ and $M_1 = M_2 = 200$ (i.e., image size: 401×401 pixels). We can obtain various versions of Mandelbrot images by changing the viewpoint of the Mandelbrot set as shown in Fig. 5. The generated Mandelbrot images contain aliasing, which prevents accurate performance evaluation of image registration algorithms. To reduce the effect of aliasing, we apply a lowpass filter to the Mandelbrot image.

5 Experiments and discussion

In this section, we describe a set of experiments for evaluating the accuracy of the proposed scale estimation algorithm using the image sequence h_t as shown in Fig. 1.

We compare the three scale estimation algorithms: (1) the conventional POC-based scale estimation algorithm [2,9] denoted by "POC," (2) algorithm (1) with the proposed iterative approach denoted by "Iterative POC" and (3) the proposed algorithm denoted by "Proposed." Algorithm (1) applies the Fourier–Mellin transform to the images, estimates the translational displacement between the transformed images using POC, and obtains the relative scale factor s_i. Algorithm (2) is an improved version of algorithm (1). We apply the proposed iterative approach as shown in Fig. 4 to algorithm (1), where Steps 3 and 4 in the proposed approach are replaced by algorithm (1). Algorithm (3) is our proposed algorithm described in Sect. 3.3.

In this experiment, we use two types of image sequences: the Mandelbrot images and the actual electron microscope images. We describe performance evaluation using Mandelbrot images and then present the experiments using the electron microscope images.

5.1 Performance evaluation using mandelbrot images

We evaluate the accuracy of the scale estimation algorithms using Mandelbrot images. As described in Sect. 4, the use of Mandelbrot images makes it possible to generate the precisely scale-controlled image sequence. In this experiment, we use Mandelbrot image sequences having the same relative scale factors $s_i^{\text{true}} = 1{,}000^{\frac{1}{T}}$ and the overall scale factor $S^{\text{true}} = 1{,}000$. In our experiment, we employ the number of stages $T = 5$–20 to evaluate the stability of the scale estimation algorithms by changing the relative scale factor s_i^{true}. Hence, the maximum relative scale factor $(T = 5)$ is 3.98, while the minimum relative scale factor $(T = 20)$ is 1.41. We estimate the relative scale factor s_i $(i = 1, \ldots, T)$ using the scale estimation algorithms, and calculate the overall scale factor $S = \prod_{i=1}^{T} s_i$. To compare the estimated overall scale factor S and the true overall scale factor S^{true}, the error [%] in estimating the overall scale factor S, which is denoted by E_T, is given by

$$E_T = \left| \frac{S}{S_{\text{true}}} - 1 \right| \times 100. \tag{12}$$

In this experiment, we use three different types of image sequences: Type A, Type B, and Type C as shown in Fig. 5.

First, we evaluate the estimation accuracy of the algorithms when the number of stages T is changed. The initial value $\tilde{s}_i$ is set to $\tilde{s}_i = s_i^{\text{true}} \times 1.05$ in this experiment, that is, the initial relative scale factor $\tilde{s}_i$ includes 5 % scale error to consider the practical situation of the electron microscope.

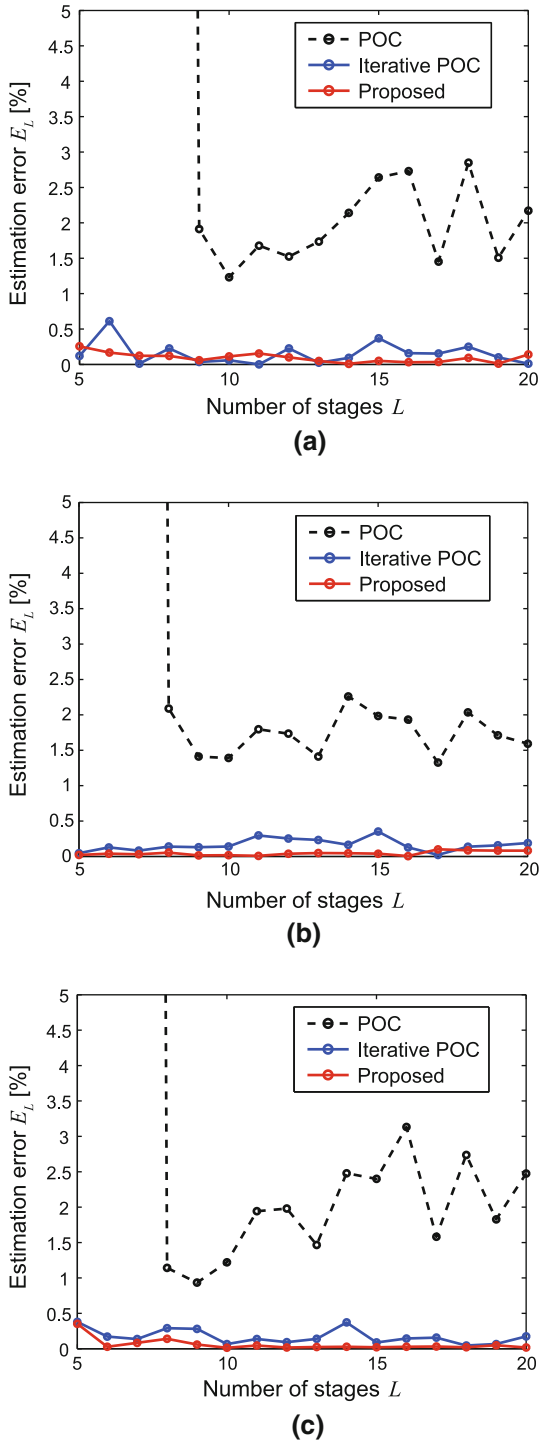

Fig. 6 Experimental results for each type of the Mandelbrot image sequence: **a** Type A, **b** Type B and **c** Type C. The POC algorithm cannot estimate the scale factor in $T < 10$, since the common region between the images is too small to estimate the scale factor. The estimation errors of the iterative POC algorithm and the proposed algorithm are lower than 0.5 % independent of the number of stages T

Figure 6 shows experimental results for each type of the Mandelbrot image sequence. The scale estimation error E_T of POC is larger than that of other algorithms. Especially, in the case of $T < 10$, i.e., $s_i^{\text{true}} > 2$, the POC algorithm cannot estimate the scale factor, since the common region between the images is too small to estimate the scale factor using POC. The estimation errors of the iterative POC algorithm and the proposed algorithm are lower than 0.5 % independent of the number of stages T. To compare the accuracy of the iterative POC and the proposed algorithms, we also evaluate the Root Mean Square (RMS) of E_T ($T = 5$–20) which indicates the inherent error of the scale estimation algorithms. Table 1 shows the RMS errors of the three algorithms for each type. The errors are around 0.15 % when using the iterative POC algorithm, while the errors are around 0.1 % when using the proposed algorithm.

Table 1 RMS errors of E_T ($T = 5$–20) for each type of the Mandelbrot image sequence

	Type A	Type B	Type C
POC	–	–	–
Iterative POC	0.0885 %	0.1747 %	0.1418 %
Proposed	0.0936 %	0.1041 %	0.0965 %

The RMS errors of POC cannot be calculated, since POC fails to estimate the relative scale factor s_i of the image sequence with $T < 10$

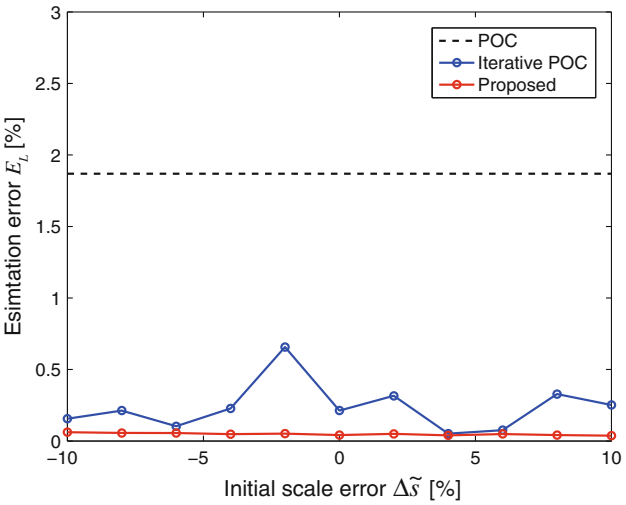

Fig. 7 Scale estimation error E_T when the initial scale error $\Delta\tilde{s}$ is changed. E_T for POC is constant, since POC dose not need an initial scale factor $\tilde{s}_i$ to estimate the scale factor s_i

Next, we evaluate the estimation accuracy of the algorithms when the initial scale error $\Delta\tilde{s}$ is changed. In the first experiment described above, we set the initial scale error $\Delta\tilde{s} = 0.05$ to perform the experiment under practical situation of the electron microscope. In this (second) experiment, the initial scale error $\Delta\tilde{s}$ is changed from -10 to 10 % with a spacing of 2 % to evaluate the robustness of the scale estimation algorithms against the initial scale error $\Delta\tilde{s}_i$. Hence, the initial relative scale factor $\tilde{s}_i$ is set to $\tilde{s}_i = s_i^{\text{true}} \times (1 + \Delta\tilde{s})$, that is, the initial relative scale fac-

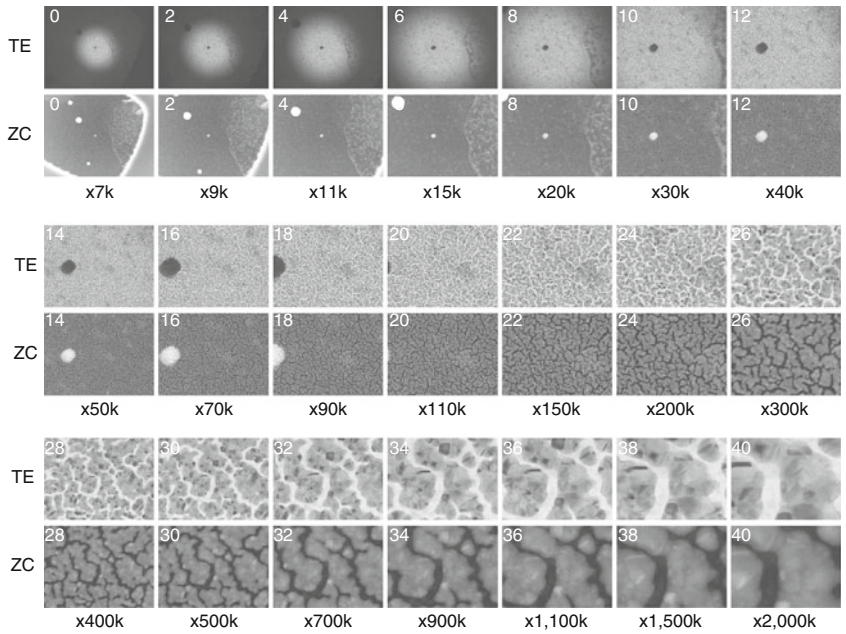

Fig. 8 Examples of electron microscope images of carbon graphite, where TE indicates the image formed by the transmission electrons, and ZC indicates the image formed by high-angle scattered electrons. We take 41 images, i.e., $T = 40$ ($t = 0 - 40$), while changing the magnification range from $\times$7,000 to $\times$2,000,000. The number on the upper left of each image indicates the image number t

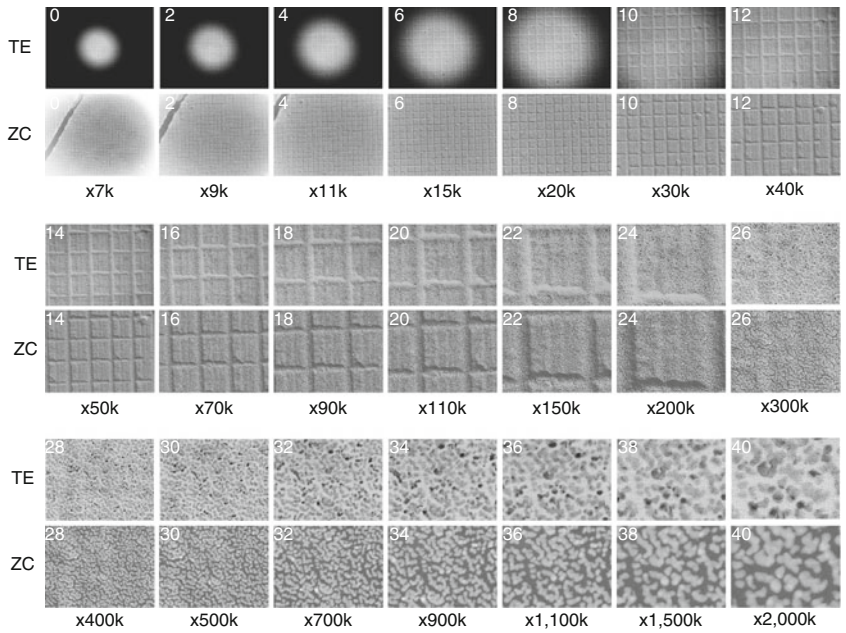

Fig. 9 Examples of electron microscope images of carbon grating, where TE indicates the image formed by the transmission electrons, and ZC indicates the image formed by high-angle scattered electrons. We take 41 images, i.e., $T = 40$ ($t = 0 - 40$), while changing the magnification range from $\times$7,000 to $\times$2,000,000. The number on the upper left of each image indicates the image number t

tor $\tilde{s}_i$ includes $\Delta\tilde{s}\%$ scale error from the true relative scale factor s_i^{true}. Note that there is no initial scale error including in $\tilde{s}_i$ when $\Delta\tilde{s} = 0$. In this experiment, we use Mandelbrot image sequence of Type A with $T = 15$. Figure 7 shows the scale estimation error E_T defined by Eq. (12) when $\Delta\tilde{s}$ is changed. Note that E_T for POC is always constant, since POC does not need the initial scale factor $\tilde{s}_i$ to estimate the relative scale factor s_i. We also evaluate the accuracy using RMS of E_T ($T = 15$ and $\Delta\tilde{s} = -0.1 - 0.1$) observed in Fig. 7. The RMS error of E_T for the iterative POC algorithm is 0.2842 %, while that for the proposed algorithm is 0.0488 %. As a result, the proposed algorithm is robust against the initial scale error $\Delta\tilde{s}$ compared with the iterative POC algorithm.

The above results clearly demonstrate the significant impact of the proposed algorithm on the accuracy of scale estimation. The proposed algorithm can estimate the overall scale factor $S = 1{,}000$ with approximately 0.1 % scale error even from the image sequences containing the initial scale error.

5.2 Experiment using electron microscope images

In this experiment, we use electron microscope images taken by a STEM (Hitachi High-Technologies HD-2000). The target objects are the carbon graphite as shown in Fig. 8 and the carbon grating as shown in Fig. 9. Setting the accelerating voltage to 200 kV, we take 41 images, i.e., $T = 40$ ($t = 0$–40), while changing the magnification range from 7,000× to 2,000,000×. The image size is 640 × 480 pixels and the relative scale factor s_i of each step is about 1.1–1.25. We get an image pair for each step using two types of detectors TE and ZC, where the image taken by TE, which is also known as the bright-field image, indicates the image formed by the transmission electrons, and the image taken by ZC, which is also known as the high-angle annular-dark-field image, indicates the image formed by high-angle scattered electrons. Note that magnifications are the same regardless of the detector types. According to this fact, we evaluate the estimation accuracy of the algorithm using the error ϵ_i [%] defined by

$$\epsilon_i = \left(\frac{s_i^{TE}}{s_i^{ZC}} - 1 \right) \times 100, \tag{13}$$

where s_i^{TE} and s_i^{ZC} are estimated relative scale factors of image sequences captured from TE and ZC, respectively. Note that the true overall scale factor S^{true} of the image sequences taken with the electron microscope is unknown. Unlike the experiments using Mandelbrot images, we evaluate the accuracy of the scale estimation algorithms using only errors in estimating the relative scale factors s_i^{TE} and s_i^{ZC}. In this experiment, we compare the accuracy of the iterative POC algorithm and the proposed algorithm.

Figure 10 shows the errors in estimated relative scale factors for image sequences of carbon graphite and carbon grating, respectively. Table 2 shows the RMS errors of each algorithm for the carbon graphite and the carbon grating. As a result, the errors of the proposed algorithm are lower than those of the iterative POC algorithm. The estimation accuracy of the iterative POC algorithm drops in high-magnification area from ×400,000 ($t = 28$) to ×2,000,000 ($t = 40$) and low-magnification area from 7,000 × ($t = 0$) to 30,000 × ($t = 10$) in Fig. 10, since the electron microscope images include substantial noise and/or have poor texture as shown in Figs. 8 and 9. On the other hand, the estimation accuracy of the proposed algorithm is stable throughout the whole sequence, since the error ϵ_i is always within −1 %∼1%. The proposed algorithm is robust against noise and blur, since the proposed algorithm selects the reliable local blocks by eliminating outliers according to the peak value of the POC function between local block images as mentioned in Sect. 3.2. The result shows that the use of the proposed algorithm makes it possible to estimate the relative scale factor s_i with 0.36 % scale error in terms of RMS

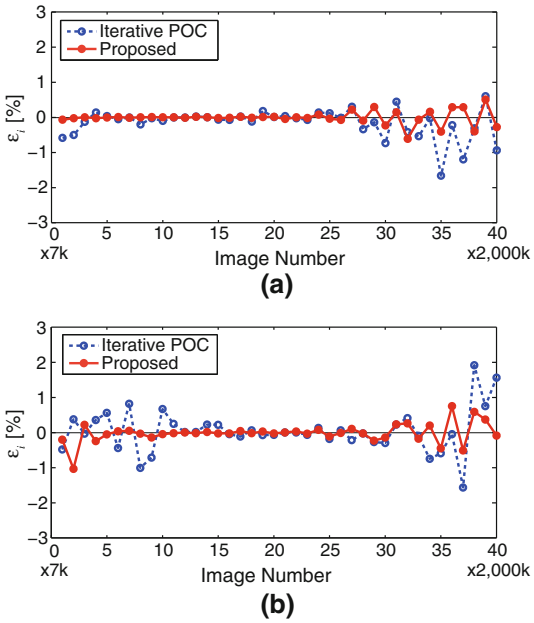

Fig. 10 Error ϵ_i [%] in estimated relative scale factors s_i^{TE} and s_i^{ZC} of **a** carbon graphite and **b** carbon grating ($i = 1$–40). The error ϵ_i defined in Eq. (13) is based on the fact that magnifications between TE and ZC are the same. The errors of the proposed algorithm are lower than those of the iterative POC algorithm. The estimation accuracy of the iterative POC algorithm drops in the high-magnification area $t = 28$–40 and the low-magnification area $t = 0$–10, since the images include substantial noise and/or have poor texture in the areas

from the actual microscope image sequences with 41 stages ($T = 40$). Since the current magnification calibration method for electron microscopes includes a maximum of 5 % scale error, the proposed algorithm demonstrates the possibility to improve the accuracy of magnification calibration of electron microscopes.

To improve the robustness of the proposed framework against the low-quality images due to noise and poor texture, we can select the high-quality images from the image sequence using the number of corresponding point pairs. As mentioned above, the corresponding point pairs are obtained only from the reliable regions having rich texture. The number of the corresponding point pairs could be used as an image quality metric for scale estimation. If the number of the corresponding point pairs between images is below a certain threshold, the input image may be eliminated as a low-quality image. Note that we have to select the high-quality images having the relative scale factor s_i below 3.98, since the proposed scale estimation algorithm can estimate the relative scale factor s_i with 0.1 %-error from the image sequence having the relative scale factor s_i between 1.41 and 3.98 from the experimental results in Sect. 5.1. Further investigation is required to demonstrate the effectiveness of the above improved framework.

Table 2 RMS errors for the carbon graphite and the carbon grating

	Carbon graphite	Carbon grating
Iterative POC	0.4408 %	0.5996 %
Proposed	0.2820 %	0.3580 %

Through the paper, we focus on geometric transformation between the electron microscope images represented by translation, rotation and scaling to estimate the relative scale factor s_t. In practice, drift distortion caused by slight movement of the object during image acquisition is also observed in the images. In the proposed framework, the accurate corresponding point pairs between the adjacent images are obtained using the phase-based correspondence matching technique. According to the corresponding point pairs, the drift distortion can be corrected by mesh-based affine transformation. In addition, the use of the accurate corresponding point pairs makes it possible to apply the proposed framework to panoramic image generation and super resolution for electron microscope images. Also, further investigation is required to confirm the applicability of the proposed framework to such applications.

6 Conclusion

This paper has proposed a high-accuracy scale estimation algorithm using phase-based correspondence matching for electron microscope images. We have also proposed a performance evaluation method using the Mandelbrot set to achieve reliable quantitative evaluation of the scale estimation algorithms. Experimental evaluation using Mandelbrot images shows that the proposed method makes it possible to estimate the overall scale factor S with approximately 0.1 % scale accuracy, where the image size is 401×401 pixels, the true overall scale factor S^{true} is 1,000, and the 10 %-initial scale error $\Delta\tilde{s}$ is included. Through experiments using the actual STEM, we demonstrate that the proposed algorithm is suitable for magnification calibration of the STEM. In our future work, we will consider a hardware implementation of the proposed algorithm on the electron microscope.

References

1. Backus, R., Williams, R.: Small spherical particles of exceptionally uniform size. J. Appl. Phys. **20**, 224–225 (1949)
2. Chen, Q., Defrise, M., Deconinck, F.: Symmetric phase-only matched filtering of Fourier–Mellin transforms for image registration and recognition. IEEE Trans. Pattern Anal. Mach. Intell. **16**(12), 1156–1168 (1994)
3. Devaney, R.L., Keen, L., Alligood, K.T.: Chaos and Fractals: The Mathematics Behind the Computer Graphics. AMS Bookstore, Providence (1989)
4. Fullam, E.: Magnification calibration of the electron microscope. J. Appl. Phys. **14**, 677–683 (1943)
5. Kuglin, C.D., Hines, D.C.: The phase correlation image alignment method. In: Proceedings of International Conference Cybernetics and Society, pp. 163–165 (1975)
6. Lowe, D.: Distinctive image features from scale-invariant keypoints. Int. J. Comput. Vis. **60**(2), 91–110 (2004)
7. Olson, N., Baker, T.: Magnification calibration and the determination of spherical virus diameters using cryo-microscopy. Ultramicroscopy **30**(3), 281–298 (1989)
8. Szeliski, R.: Computer Vision: Algorithms and Applications. Springer, Berlin (2010)
9. Takita, K., Aoki, T., Sasaki, Y., Higuchi, T., Kobayashi, K.: High-accuracy subpixel image registration based on phase-only correlation. IEICE Trans. Fundam. **E86-A**(8), 1925–1934 (2003)
10. Takita, K., Muquit, M.A., Aoki, T., Higuchi, T.: A sub-pixel correspondence search technique for computer vision applications. IEICE Trans. Fundam. **E87-A**(8), 1913–1923 (2004)
11. van der Laak, J.A.W.M., Dijkman, H.B.P.M., Pahlplatz, M.M.M.: Automated magnification calibration in transmission electron microscopy using Fourier analysis of replica images. Ultramicroscopy **106**(4–5), 255–260 (2006)
12. Wrigley, N.: The lattice spacing of crystalline catalase as an internal standard of length in electron microscopy. J. Ultrastruct. Res. **24**, 454–464 (1968)
13. Zhao, F., Yang, Y.: Use of monodisperse gold nanoperticles for transmission electron microscope high magnification calibration. Colloid J. **72**(3), 346–352 (2010)

Author Biographies

Koichi Ito received the B.E. degree in electronic engineering, and the M.S. and Ph.D. degree in information sciences from Tohoku University, Sendai, Japan, in 2000, 2002 and 2005, respectively. He is currently an Assistant Professor of the Graduate School of Information Sciences at Tohoku University. From 2004 to 2005, he was a Research Fellow of the Japan Society for the Promotion of Science. His research interest includes signal and image processing, and biometric authentication.

Ayako Suzuki received the B.E. degree in information engineering, and the M.S. degree in information sciences from Tohoku University, Sendai, Japan, in 2009 and 2011, respectively. She is currently working at IT Platform Integration Division, Nomura Research Institute, Ltd. Her research interest includes image processing, and machine vision.

Takafumi Aoki received the B.E., M.E., and D.E. degrees in electronic engineering from Tohoku University, Sendai, Japan, in 1988, 1990, and 1992, respectively. He is currently a professor in the Graduate School of Information Sciences (GSIS) at Tohoku University. In April 2012, Aoki was appointed as the Vice President of Tohoku University. His research interests include theoretical aspects of computation, computer design and organization, LSI systems for embedded applications, digital signal processing, computer vision, image processing, biometric authentication, and security issues in computer systems. He received more than 20 academic awards, including the IEE Ambrose Fleming Premium Award (1994), the IEE Mountbatten Premium Award (1999), the IEICE Outstanding Transaction Paper Awards (1989 and 1997), the IEICE Inose Award (1997), the Ichimura Award (2008), as well as many outstanding paper awards from international conferences and symposiums such as ISMVL, ISPACS, SASIMI and COOL Chips.

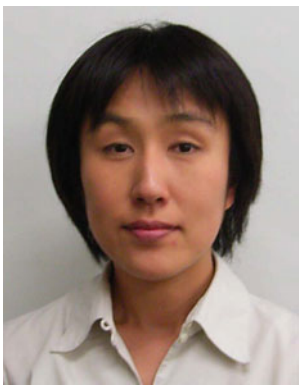

Ruriko Tsuneta received the B.S. and the M.S. degrees in engineering from Hokkaidou University, Japan, in 1989 and 1991, respectively. She joined the Central Research Laboratory, Hitachi Ltd., Tokyo in 1991, where she has been developing transmission electron microscopy.